



HAL
open science

Influence of sodium borate on the early age hydration of calcium sulfoaluminate cement

Jean-Baptiste Champenois, Mélanie Dhoury, Céline Cau Dit Coumes, Cyrille Albert-Mercier, Bertrand Revel, Patrick Le Bescop, Denis Damidot

► **To cite this version:**

Jean-Baptiste Champenois, Mélanie Dhoury, Céline Cau Dit Coumes, Cyrille Albert-Mercier, Bertrand Revel, et al.. Influence of sodium borate on the early age hydration of calcium sulfoaluminate cement. Cement and Concrete Research, 2015, 70, pp.83-93. 10.1016/j.cemconres.2014.12.010 . hal-03116356

HAL Id: hal-03116356

<https://uphf.hal.science/hal-03116356v1>

Submitted on 14 Jan 2025

HAL is a multi-disciplinary open access archive for the deposit and dissemination of scientific research documents, whether they are published or not. The documents may come from teaching and research institutions in France or abroad, or from public or private research centers.

L'archive ouverte pluridisciplinaire **HAL**, est destinée au dépôt et à la diffusion de documents scientifiques de niveau recherche, publiés ou non, émanant des établissements d'enseignement et de recherche français ou étrangers, des laboratoires publics ou privés.

Influence of sodium borate on the early age hydration of calcium sulfoaluminate cement

Jean-Baptiste Champenois^a, Mélanie Dhoury^a, Céline Cau Dit Coumes^{a,*}, Cyrille Mercier^b, Bertrand Revel^c, Patrick Le Bescop^d, Denis Damidot^e

^a CEA, DEN, DTCD, SPDE, F-30207 Bagnols-sur-Cèze Cedex, France

^b LMCPA, Université de Valenciennes et du Hainaut Cambrésis, 59600 Maubeuge, France

^c Centre Commun de Mesure RMN, Université Lille1 Sciences Technologiques, Cité Scientifique, 59655 Villeneuve d'Ascq Cedex, France

^d CEA, DEN, DPC, SECR, F-91192 Gif-sur-Yvette, France

^e Ecole des Mines de Douai, LGCgE-GCE, 59508 Douai, France

ABSTRACT

Calcium sulfoaluminate (CSA) cements are potential candidates for the conditioning of radioactive wastes with high sodium borate concentrations. This work thus investigates early age hydration of two CSA cements with different gypsum contents (0 to 20%) as a function of the mixing solution composition (borate and NaOH concentrations). Gypsum plays a key role in controlling the reactivity of cement. When the mixing solution is pure water, increasing the gypsum concentration accelerates cement hydration. However, the reverse is observed when the mixing solution contains sodium borate. Until gypsum exhaustion, the pore solution pH remains constant at ~10.8, and a poorly crystallized borate compound (ulexite) precipitates. A correlation is established between this transient precipitation and the hydration delay. Decreasing the gypsum content in the binder, or increasing the sodium content in the mixing solution, are two ways of reducing the stability of ulexite, thus decreasing the hydration delay.

Keywords:

Hydration (A)

Retardation (A)

Sulfoaluminate (D)

Waste management (E)

1. Introduction

Calcium sulfoaluminate (CSA) cements requiring less energy and producing less CO₂ than Portland cement during their manufacture are receiving increasing attention in the context of sustainable development [1,2]. They can have highly variable compositions, but all of them contain ye'elimite, also called Klein's compound, in their clinker [3–6]. In this article, we will consider only sulfoaluminate belite cements in which ye'elimite (C₄A₃S̄¹) predominates over belite (C₂S) [7]. A wide range of gypsum or anhydrite contents (typically from 10 to 25% for gypsum) can be ground with CSA clinker to produce different CSA cements, ranging from rapid-hardening (at low gypsum content) to shrinkage-compensating, and eventually to self-stressing (at high gypsum content) [8]. Besides, CSA cements are of interest to stabilize hazardous wastes [9–15]. It has been shown recently that belite calcium sulfoaluminate cements with high ye'elimite contents may have good potential for the conditioning of borate-containing radioactive wastes: their rate of hydration is less retarded by borate ions than that of ordinary Portland cement [16–19]. Besides, they form by hydration

large amounts of AFm and AFt phases [20–24]. However, the mechanism by which concentrated sodium borate solutions modify the hydration of CSA cements is still not fully understood. The speciation of boron in the cement paste also needs some clarifications. In addition to the AFm and AFt phases, other borate minerals can potentially form at high pH in the presence of calcium (frolovite CBH₄, hexahydroborite CBH₆, C₂BH, C₂B₃H₈, inyoite C₂B₃H₁₃ and nobleite CB₃H₄) [25–28]. Moreover, since the concentrated borate waste contains sodium, sodium borates should also be considered (NBH₈, NB₂H₁₀, NB₅H₁₀), as well as a mixed borate mineral containing sodium and calcium (ulexite NC₂B₅H₁₆) [25].

This work aims at giving new insight into the influence of sodium borate on the early age hydration of calcium sulfoaluminate cements with variable gypsum contents, as well as on the processes involved. A better understanding of the chemical evolution of such systems will help optimize the CSA cement-based recipes developed for the conditioning of radioactive borate-containing waste.

2. Experimental

2.1. Materials and specimen preparation

Several CSA cements were prepared by mixing a ground industrial CSA clinker (Belitex KTS 100) (d₁₀ = 2.5 μm, d₅₀ = 15.1 μm, d₉₀ =

* Corresponding author.

E-mail address: celine.cau-dit-coumes@cea.fr (C. Cau Dit Coumes).

¹ Shorthand cement notations are used in this article: C = CaO, S = SiO₂, S̄ = SO₃, A = Al₂O₃, H = H₂O, T = TiO₂, B = B₂O₃ and N = Na₂O.

Table 1
Mineralogical composition of CSA clinker.

Minerals	C ₄ A ₃ S	C ₂ S	C ₁₂ A ₇	CT	MgO	Others
Weight %	66.2	13.5	9.4	2.6	0.9	7.4

49.8 μm, BET specific surface area = 4.8 m²/g) with the appropriate amount (0% to 20% by weight of cement) of analytical grade gypsum (d₁₀ = 5.4 μm, d₅₀ = 18.7 μm, d₉₀ = 52.4 μm, BET specific surface area ~0.5 m²/g) for 15 min. The mineralogical composition of the CSA clinker is reported in Table 1. In the clinker, ye'elimite predominated over belite and mayenite. The other minor constituents, mainly phases containing titanium and iron, could be regarded as hydraulically inactive.

Cement pastes were prepared using a water to cement (w/c) ratio of 0.6. There were two main reasons for choosing such a high ratio.

- It should be noted that the chemical water demand of CSA cements is higher than that of Portland cement, and increases with the gypsum content of the binder [8]. In a previous work [29], it was shown that the minimum amount of water required for total hydration of cement comprising 80% clinker and 20% gypsum corresponds to a w/c ratio of 0.59 (0.54 by taking into account water brought by gypsum). The w/c ratio of 0.6 thus resulted from a compromise to avoid any stop in the hydration process due to lack of water while preventing any bleeding at an early age.
- From a more applied point of view, in the waste stabilization process, water is only brought by the waste. The higher the water content, the higher the waste loading in the cement matrix.

The mixing solution was either demineralized water or a solution containing 1 mol/L of borate ions at pH 11. In the latter case, the appropriate amount of boric acid was dissolved in demineralized water and the pH was set to 11 by adding analytical grade sodium hydroxide (960 mmol/L of NaOH for 1 mol/L of H₃BO₃). Such a solution mimics some contaminated waste streams generated by PWR nuclear plants. In the second part of the study, the sodium hydroxide concentration was varied from 0.85 mol/L to 1.12 mol/L while keeping the boric acid concentration constant at 1 mol/L, in order to get different pH values.

Mixing was performed for 5 min using a laboratory mixer equipped with an anchor stirrer and rotating at 100 r.p.m. Cement pastes were cast into airtight polypropylene boxes (7 mL of paste per box), and cured at 20 °C.

2.2. Specimen characterization

Hydration of the cement pastes was investigated using a highly sensitive Setaram C80-type microcalorimeter under isothermal conditions at 25 °C.

Cement hydration was also stopped after fixed periods of time, depending on the samples, by successively immersing the crushed paste into isopropanol and drying it in a controlled humidity chamber (with 20% relative humidity at 22 ± 2 °C). Crystallized phases were identified by X-ray diffraction with the Bragg Brentano geometry (Siemens D8 – copper anode λK_{α1} = 1.54056 Å generated at 40 mA and 40 kV) on pastes ground by hand to a particle size of less than 100 μm. Before analysis, silicon was added to the samples (10% by mass of sample) and carefully mixed by grinding in a mortar to be used as an internal standard. The evolutions of the amounts of ettringite, monosulfate, gypsum, mayenite, ye'elimite, and of the boro-AfT phase were assessed from the XRD patterns by measuring the areas of characteristic reflections, standardized with respect to that of silicon (2θ = 9.08° for ettringite, 9.93° for monosulfate, 11.64° for gypsum, 33.42° for mayenite, 23.67° and 23.70° for ye'elimite, 9.2° for the boro-AfT phase, and 28.44° for silicon). Four test mixtures containing known fractions of clinker and gypsum were analyzed using this method. The error on the determination of the ye'elimite and gypsum contents ranged between 5 and 10%. Thermogravimetric analyses were carried out using a TGA/DSC Netzsch STA 409 PC instrument at 10 °C/min up to 1000 °C.

Some cement paste samples were characterized using ¹¹B-MAS NMR. The ¹¹B-MAS spectra were recorded at a Larmor frequency of 256.7 MHz using a Bruker Avance III 800 MHz (18.8 T) spectrometer. The spectra were made up of 64 free induction decays with a pulse length of 1 μs (π/10) and a relaxation delay of 5 s. The samples were spun at 20 kHz in a 3.2 mm probe. Experimental referencing, calibration, and setup were performed using solid powdered sodium borohydride. Solid NaBH₄ has a chemical shift of –42.06 ppm relative to the primary standard, liquid F₃B·O(C₂H₅)₂ (where δ(¹¹B) = 0.00 ppm). The baseline was corrected by subtracting the background signal coming from the boron nitride stator of the probe. Spectral decomposition was performed using DMFit software [30].

The pore solution of the cement pastes was also extracted by compaction of 20 mL of sample using a Carver mechanical press at a pressure of 34 MPa. Its pH was then measured with a high-alkalinity electrode (Mettler Toledo Inlab Expert Pt1000 pH 0–14 T 0–100 °C) calibrated using three IUPAC pH buffers at 6.865 ± 0.010 (25 °C), 10.012 ± 0.010 (25 °C) and 12.45 ± 0.05 (25 °C) and its chemical composition

Table 2
Boron containing aqueous species and minerals added to the Cemdata07 database.

Species	Formation reaction	Log K (T = 25 °C, P = 1 bar)	Ref.	
Aqueous	B(OH) ₄ [−]	B(OH) _{3(aq)} + H ₂ O → B(OH) ₄ [−] + H ⁺	−9.24	[43–47]
	B ₃ O ₃ (OH) ₄ [−]	3B(OH) _{3(aq)} → B ₃ O ₃ (OH) ₄ [−] + H ⁺ + 2H ₂ O	−7.21	[33,48]
	B ₅ O ₆ (OH) ₄ [−]	5B(OH) _{3(aq)} → B ₅ O ₆ (OH) ₄ [−] + H ⁺ + 5H ₂ O	−7.01	[33,48]
	B ₄ O ₅ (OH) ₄ ^{2−}	4B(OH) _{3(aq)} → B ₄ O ₅ (OH) ₄ ^{2−} + 2H ⁺ + 3H ₂ O	−15.89	[33,49–51]
	Al(OH) ₃ OB(OH) ₂ [−]	B(OH) _{3(aq)} + Al ³⁺ + 3H ₂ O → Al(OH) ₃ OB(OH) ₂ [−] + 4H ⁺	−21.26	[52,55]
	NaB(OH) ₄ (aq)	B(OH) _{3(aq)} + Na ⁺ + H ₂ O → NaB(OH) ₄ (aq) + H ⁺	−8.91	[33,53]
	CaB(OH) ₄ ⁺	B(OH) _{3(aq)} + Ca ²⁺ + H ₂ O → CaB(OH) ₄ ⁺ + H ⁺	−7.42	[53,54]
	Hexahydroborite	2B(OH) _{3(aq)} + Ca ²⁺ + 6H ₂ O → Hexahydroborite + 2H ⁺	−13.65	[25–28,54]
	Boric acid	B(OH) _{3(aq)} → boric acid	0.0438	[33]
	Inyoite	6B(OH) _{3(aq)} + 2Ca ²⁺ + 6H ₂ O → Inyoite + 4H ⁺	−19.72	[25–28,54]
Minerals	Borax	4B(OH) _{3(aq)} + 2Na ⁺ + 5H ₂ O → Borax + 2H ⁺	−24.80	[25–28,54]
	Na ₂ O·B ₂ O ₃ ·8H ₂ O	2B(OH) _{3(aq)} + 2Na ⁺ + 4H ₂ O → Na ₂ O·B ₂ O ₃ ·8H ₂ O + 2H ⁺	−18.55	[25–28,54]
	Nobleite	6B(OH) _{3(aq)} + Ca ²⁺ → Nobleite + 2H ⁺ + 3H ₂ O	−7.75	[25–28,54]
	Sborgite	10B(OH) _{3(aq)} + 2Na ⁺ → Sborgite + 2H ⁺ + 4H ₂ O	−8.985	[25–28,54]
	Ulexite	10B(OH) _{3(aq)} + 2Na ⁺ + 2Ca ²⁺ + 4H ₂ O → Ulexite + 6H ⁺	−28.50	[25–28,54]
	4Boro-AfT	4B(OH) _{3(aq)} + 2Al ³⁺ + 6Ca ²⁺ + 42H ₂ O → Boro-AfT + 18H ⁺	−123.80	[24,33]
	Boro-AFm	B(OH) _{3(aq)} + 2Al ³⁺ + 4Ca ²⁺ + 17.5H ₂ O → Boro-AFm + 14H ⁺	−95.83	[24,33]
	U phase	1.8Al ³⁺ + 4Ca ²⁺ + Na ⁺ + 1.1SO ₄ ^{2−} + 16.5H ₂ O → U phase + 12.2H ⁺	−78.96	[37]
	Ye'elimite	4Ca ²⁺ + 6Al ³⁺ + SO ₄ ^{2−} + 12H ₂ O → Ye'elimite + 24H ⁺	−350 ^a	

^a Arbitrary value allowing full dissolution of ye'elimite under the investigated conditions.

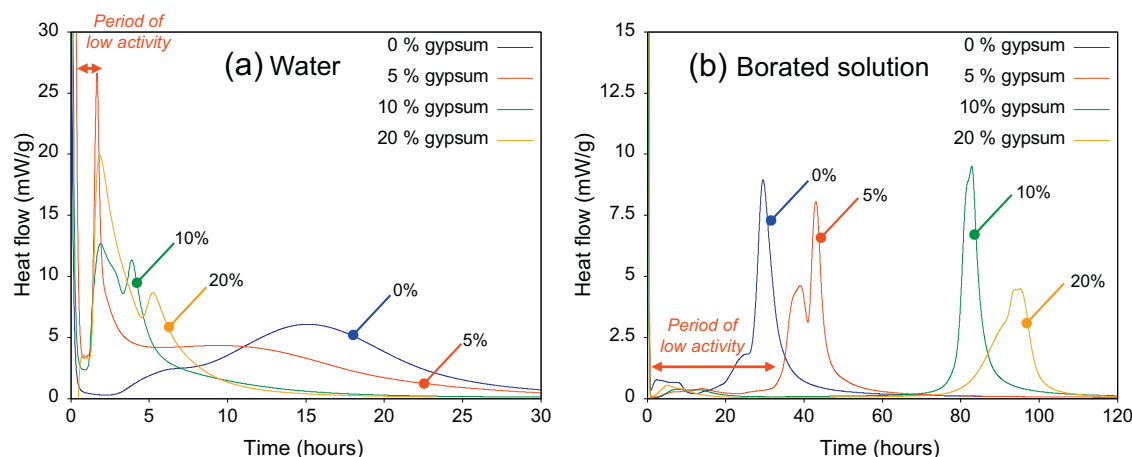


Fig. 1. Influence of the initial gypsum content on the heat produced during CSA cement hydration in the presence of demineralized water (a), or of a borate-containing solution (b) ($[B]_{\text{tot}} = 1 \text{ mol/L}$, $\text{pH} = 11$, $w/c = 0.6$) under isothermal conditions ($T = 25 \text{ }^\circ\text{C}$).

was determined using ICP-OES (Vista Pro Varian – standardization with matrix reconstitution). The analytical error was $\pm 5\%$.

2.3. Ulexite synthesis

Ulexite was synthesized by mixing calcium hydroxide and boric acid in demineralized water with a B/Ca molar ratio of 9. The pH was then set to 10 by the addition of sodium hydroxide. A white and gel-like compound precipitated instantaneously. The product was very sensitive to dehydration. Its X-ray diffraction pattern was recorded using the Debye Scherer geometry (transmission mode). The suspension (precipitated product + solution) was introduced in a Lindeman tube ($\Phi = 1 \text{ mm}$) which was tightly closed and mounted on a spinning goniometric head during measurement to reduce the preferred orientation effect. Data were recorded by using copper radiation ($\lambda = 1.5418 \text{ \AA}$) at room temperature in a 2θ range of $4\text{--}120^\circ$ with a step size of 0.011° for a total counting time of 8 h. The product morphology was also observed after filtration, rinsing with demineralized water and gentle drying at $30 \text{ }^\circ\text{C}$ using SEM (ESEM Quanta 50 FEI microscope equipped with a thermal field emission gun) in the environmental mode at $5 \text{ }^\circ\text{C}$ and 650 Pa (which corresponded to a relative humidity close to 95%). Its chemical composition was determined by ICP-OES analysis. The powder was dissolved in a small volume of concentrated nitric acid (1 mol/L), and the resulting solution was analyzed for Ca, Na, and B using ICP-OES (Vista Pro Varian, standardization with matrix reconstitution, analytical error $\pm 5\%$). Finally, the powder was also characterized using ^{11}B -MAS NMR according to the protocol described in Section 2.2.

2.4. Thermodynamic modeling

Experiments were supported by thermodynamic equilibrium modeling in order to predict the evolution of the mineralogy and pore solution composition of the cement pastes with ongoing hydration. Thermodynamic calculations were carried out using the CHESSE software which works by minimizing the free energy of a pre-defined system [31].

The quality of modeling directly depends on the quality and completeness of the underlying database [32]. A review of the literature was thus performed to identify the boron-containing aqueous species and minerals relevant to the investigated systems [33]. They are summarized in Table 2, together with their formation constants. These data were added to the Cemdata07 database which contains thermodynamic data for a number of cement phases [34].

Different forms of aluminum hydroxide were tested in the thermodynamic model. With gibbsite ($\text{Al}^{3+} + 3\text{H}_2\text{O} \rightarrow \text{Al}(\text{OH})_3 + 3\text{H}^+$, $\log K = -7.756$ at $25 \text{ }^\circ\text{C}$) and bayerite ($\log K = -8.6$ at $25 \text{ }^\circ\text{C}$), the simulations fitted well with the experiments (prediction of the phase assemblage and pH evolution). This was not the case for amorphous aluminum hydroxide ($\log K = -9.1282$ at $25 \text{ }^\circ\text{C}$). Since the analysis by XRD of cement pastes aged 3 months and 1 year showed the presence of broad peaks corresponding to poorly crystallized gibbsite, this form was selected for the subsequent calculations.

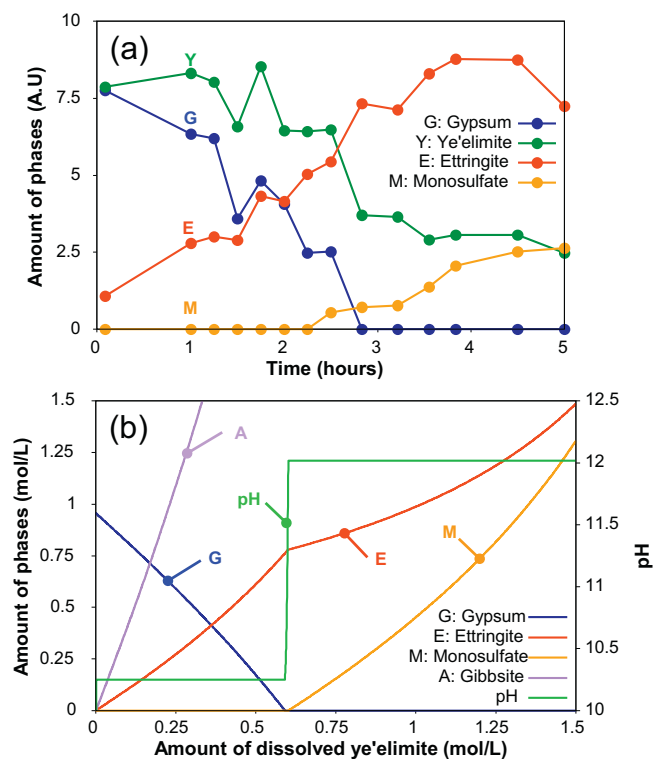


Fig. 2. Hydration of a CSA cement with 10% gypsum (which corresponds to a concentration of 970 mmol/L in the mixing water) in the presence of water ($w/c = 0.6$; $T = 20 \text{ }^\circ\text{C}$). (a) Semi-quantitative evolution of the mineralogy inferred from XRD analysis. (b) Thermodynamic modeling of the hydrate assemblage formed by the progressive dissolution of ye'elimite in an aqueous suspension initially containing 970 mmol/L of gypsum.

3. Results and discussion

3.1. Heat production during cement hydration (conduction calorimetry)

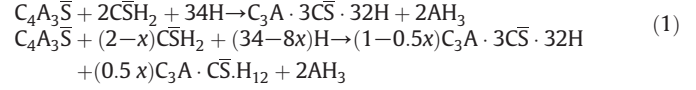
The heat flux released during CSA cement hydration in the presence of demineralized water or of a borate-containing solution ($[B] = 1 \text{ mol/L}$, $\text{pH} = 11$) was investigated using isothermal microcalorimetry ($T = 25 \text{ }^\circ\text{C}$) as a function of the initial gypsum content of the binder.

3.1.1. Hydration in the presence of pure water

When the mixing solution was pure water (Fig. 1-a), the heat flow exhibited a first maximum just after the water addition, which resulted from very early hydration reactions [35]. This heat output was too rapid to be recorded with the type of calorimeter used in this study, and the signal measured during the first 30 min was rather due to extra undesirable heat caused by the sample introduction in the calorimetric chamber. It was followed by a period of low thermal activity, corresponding to the slow dissolution of anhydrous phases and slow precipitation of cement hydrates at the surface of the cement grains (mainly ettringite and amorphous aluminum hydroxide) [29].

Afterwards, the heat flow increased again, indicating a strong acceleration of hydration, and reached a second maximum before decreasing. In agreement with previous results [29,35,36], this heat event, responsible for setting of the paste, comprised at least two periods, as shown by the shoulder on the left or right-side of the peak. In the first period, the consumption of ye'elimite accelerated and ettringite precipitated

together with aluminum hydroxide according to Eq. (1). The second period resulted from a deficit in gypsum, leading to the formation of a mix of monosulfate and ettringite, for instance according to the balanced Eq. (2).



$$\text{with } 0 < x \leq 2. \quad (2)$$

The initial gypsum content of the binder not only influenced this change in the thermal regime, but also the duration of the period of low thermal activity. It was enhanced by the absence of gypsum, as already noticed by Berger et al. [13].

3.1.2. Hydration in the presence of a sodium borate solution

On the contrary, when the mixing solution contained borates, decreasing the gypsum content shortened the period of low activity (Fig. 1-b). For instance, the heat flux reached its maximum after 28 h for a gypsum-free binder, instead of about 80 h for a binder with 10% gypsum. Borate ions also retarded hydration of the CSA cements whatever their gypsum content. In comparison, the maximum heat fluxes of reference samples prepared with water were indeed recorded at 12 h only in the absence of gypsum, and at about 3 h with 10% gypsum. It should be noted however that the retardation caused by borate ions

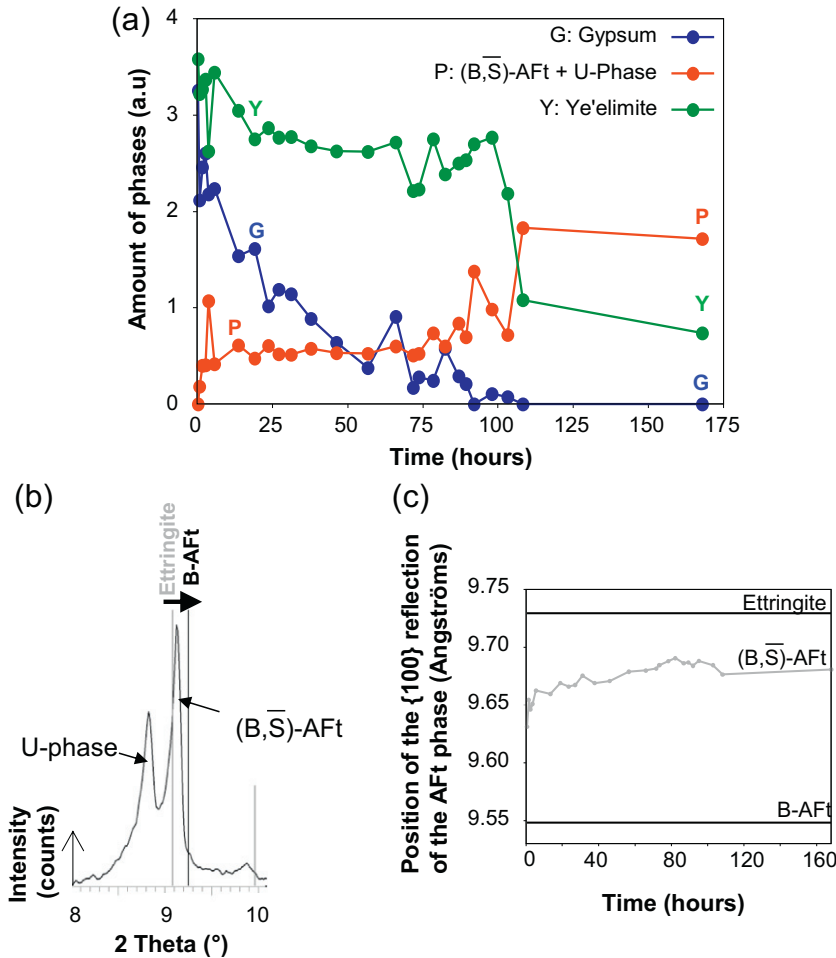


Fig. 3. Hydration of a CSA cement with 10% gypsum in the presence of a sodium borate solution ($[B]_{\text{tot}} = 1 \text{ mol/L}$, $\text{pH} = 11$, $w/c = 0.6$; $T = 20 \text{ }^\circ\text{C}$). (a) Semi-quantitative evolution of the mineralogy inferred from XRD analysis. (b) Shift of the {100} reflection of the precipitated AFt-type phase compared to ettringite and B-AFt. (c) Evolution of the position of the {100} reflection of the $(\text{B}, \bar{\text{S}})\text{-AFt}$ phase during hydration.

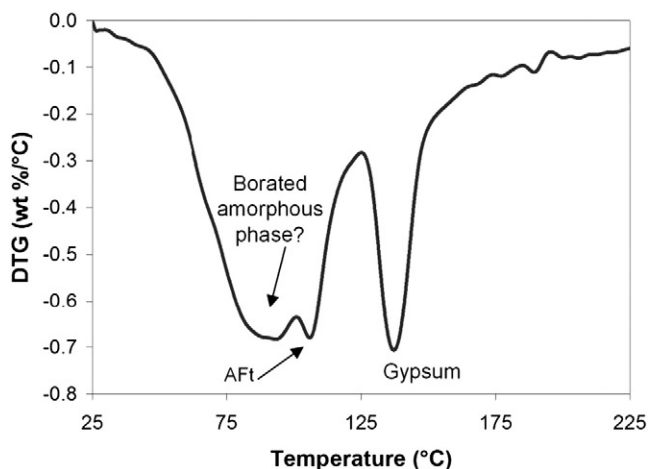


Fig. 4. Hydration of a CSA cement with 10% gypsum in the presence of a sodium borate solution ($[B]_{\text{tot}} = 1 \text{ mol/L}$, $\text{pH} = 11$, $w/c = 0.6$; $T = 20 \text{ }^\circ\text{C}$): TGA analysis of a 24 h-old sample.

was much lower for CSA cements than for Portland cement (OPC): under similar conditions, the maximum heat flux occurred after about 140 h for OPC [19].

3.2. Phase assemblage and pore solution chemistry during cement hydration

The previous results raised some questions about the way borate ions retarded CSA cement hydration, and about the variable effect of gypsum on the early stages of CSA cement hydration depending on the composition of the mixing solution. The evolution of the mineralogy and pore solution composition with ongoing hydration was thus carefully investigated for two specimens prepared with CSA cement

comprising 10% gypsum and water (reference) or the borate-containing solution ($[B]_{\text{tot}} = 1 \text{ mol/L}$, $\text{pH} = 11$).

3.2.1. Hydration in the presence of pure water

As expected, the main crystallized hydrate precipitated in the reference sample was ettringite as long as there was enough gypsum in the system (Fig. 2-a). Then, monosulfate formed. Aluminum hydroxide precipitated in an amorphous form and was not detected by XRD, but could be identified from the first characterization time by TGA due to its water loss at $275 \text{ }^\circ\text{C}$. The extracted pore solution had a pH of 10.5 until gypsum exhaustion. Then, the pH increased to 12. These results were fairly well reproduced by thermodynamic calculations simulating the hydration of a simplified mixture of ye'elimite and gypsum (Fig. 2-b).

3.2.2. Hydration in the presence of a sodium borate solution

Adding sodium borate to the mixing solution had a strong influence on the evolution of the mineralogy during the early age hydration. The XRD patterns recorded up to 95 h showed that very few amounts of ye'elimite dissolved until the depletion of gypsum (Fig. 3-a). Note that the heat flow peak accompanying the acceleration of hydration was recorded about 10 h earlier in the calorimetric experiment (Fig. 1-b). However, the samples for the mineralogical investigation were cured at $20 \text{ }^\circ\text{C}$, instead of $25 \text{ }^\circ\text{C}$ for the calorimetric study. This temperature difference could explain the slightly different rates of hydration in the two experiments since it is well known that CSA cement hydration is highly thermo-sensitive [29]. Consumption of mayenite was difficult to assess from the XRD patterns because its diffraction lines had a weak intensity and overlapped with those of other minerals (ye'elimite, AFt phase).

The slow dissolution of ye'elimite was accompanied by the precipitation of an AFt-type phase. Its {100} reflection exhibited a small deviation towards higher angles as compared with pure ettringite (Fig. 3-b). This could be explained by the partial substitution of sulfate anions by borate anions in the structure of ettringite. Wenda and Kuzel [20] showed indeed that borate can completely substitute for sulfate in AFt phases. Poellmann et al. [23] additionally demonstrated that a large

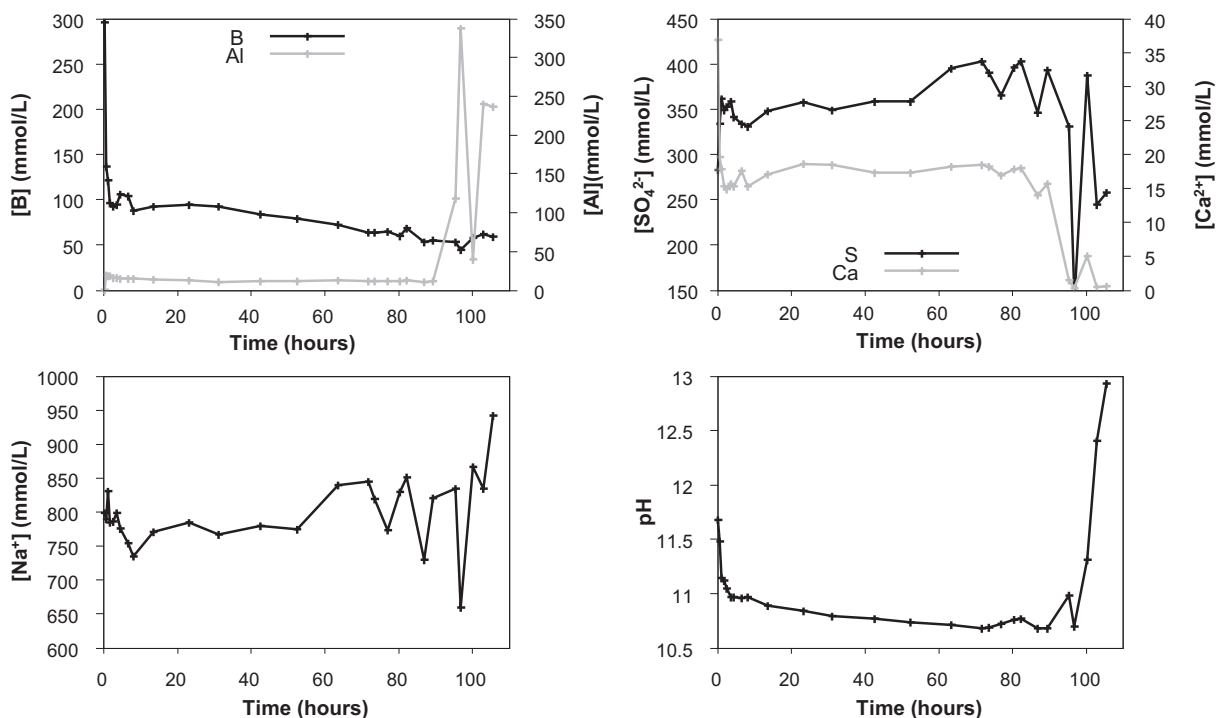


Fig. 5. Hydration of a CSA cement with 10% gypsum in the presence of a sodium borate solution ($[B]_{\text{tot}} = 1 \text{ mol/L}$, $\text{pH} = 11$, $w/c = 0.6$, $T = 20 \text{ }^\circ\text{C}$): evolution of pH and composition of the pore solution during hydration.

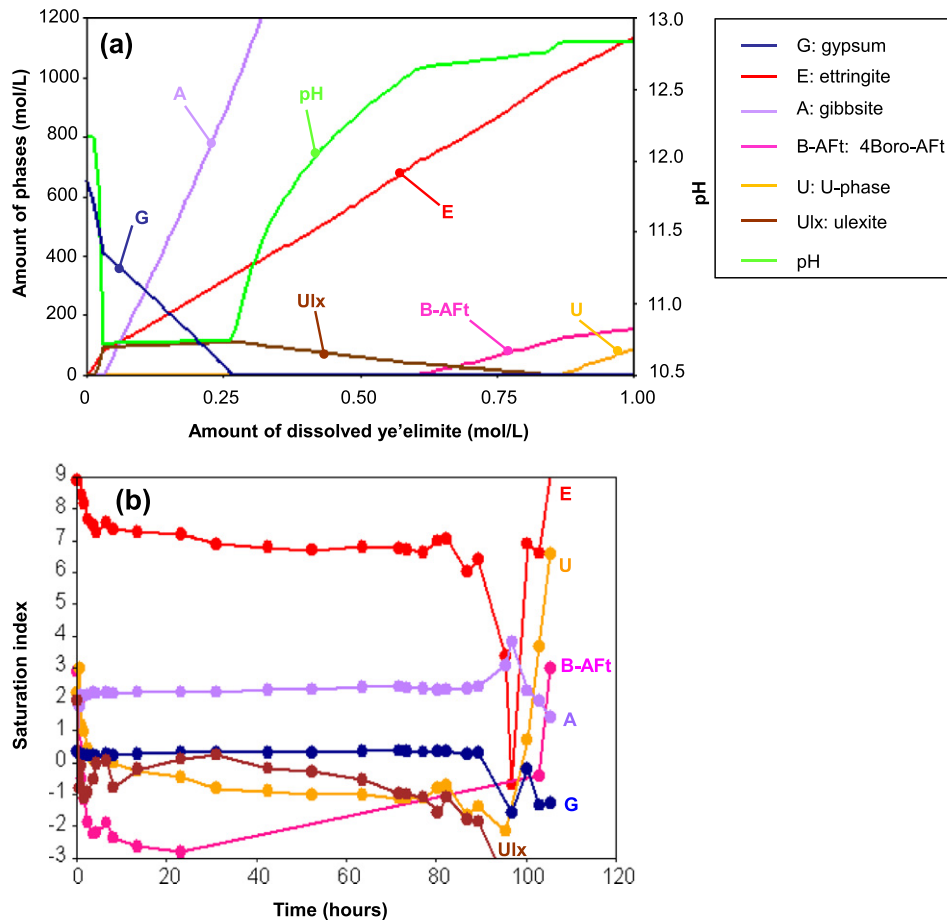


Fig. 6. Thermodynamic investigation of the hydration of a CSA cement with 10% gypsum (corresponding to 970 mmol/L in the mixing solution) in the presence of a sodium borate solution ($[B]_{\text{tot}} = 1 \text{ mol/L}$, $[\text{NaOH}] = 960 \text{ mmol/L}$). (a) Modeling of the hydrate assemblage formed by the progressive dissolution of ye'elimite in an aqueous suspension initially containing 970 mmol/L of gypsum, 1 mol/L of H_3BO_3 , and 960 mmol/L of NaOH. (b) Evolution of the saturation indexes of the main hydrates during hydration of the CSA cement paste (calculations based on the experimental concentrations measured in the pore solution).

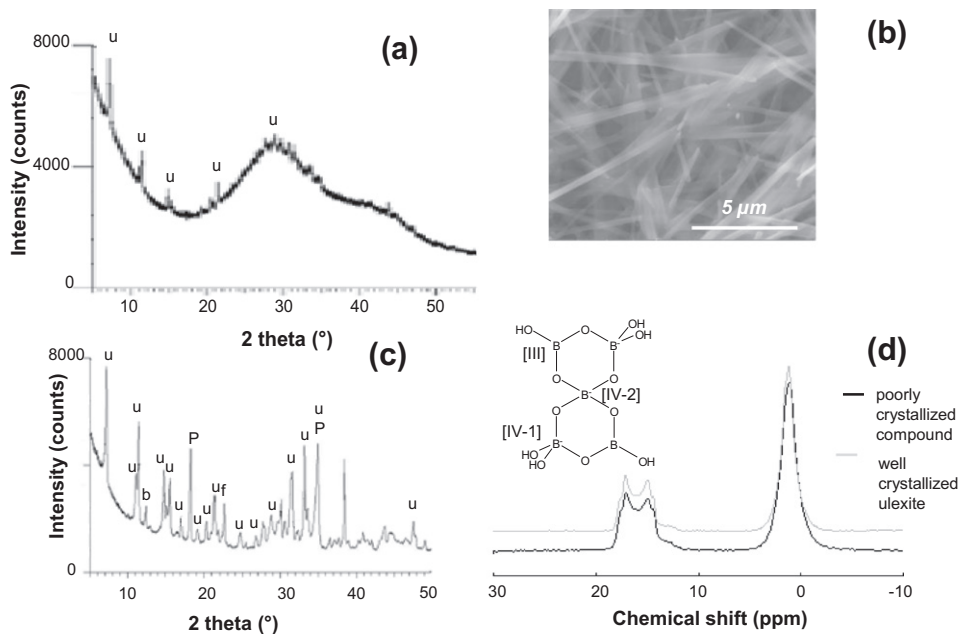


Fig. 7. Characterization of ulexite. (a) X-ray diffraction pattern of the poorly crystallized product obtained by coprecipitation. (b) Morphology of the poorly crystallized product observed by ESEM. (c) X-ray diffraction pattern of the product after drying with isopropanol (u: ulexite, P: portlandite, b: pentahydroborite (CBH_5), f: frolovite (CBH_4)). (d) Comparison of the ^{11}B -MAS NMR spectra of well-crystallized ulexite and poorly crystallized product obtained by coprecipitation – structure of borate groups in the structure of ulexite. From [28].

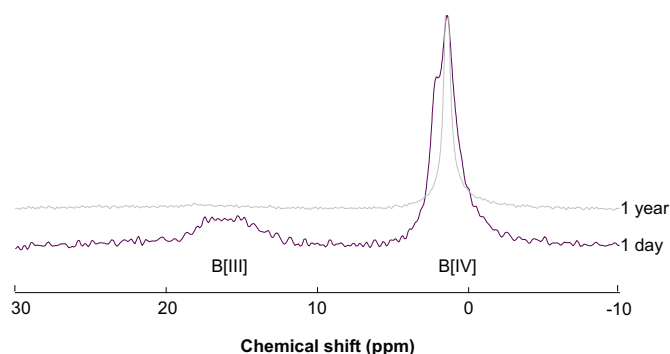


Fig. 8. ^{11}B -MAS NMR spectra of the cement paste hydrated in the presence of the sodium borate solution.

range of solid solutions exists between ettringite and the AFt phase containing boron. When the hydration degree increased, the amount of AFt-type phase increased, and the angular position of its {100} reflection approached that of pure ettringite (Fig. 3-c), which could be explained by the progressive release of sulfates by the dissolution of the anhydrous phases. When gypsum was exhausted, the massive dissolution of ye'elimite occurred, accompanied by the massive precipitation of the AFt-type phase. Small amounts of U-phase were also evidenced by XRD. It is an AFm-type phase, similar to monosulfate, where some calcium cations are substituted by sodium cations [37]. Its precipitation could be expected given the very high concentration of sodium (960 mmol/L) in the mixing solution due to the pH set to 11 with sodium hydroxide. No other AFm-type phases could be detected.

Thermogravimetry analysis performed on a 1d-old paste confirmed the presence of residual gypsum and of small amounts of an AFt-type phase (Fig. 4). An additional important weight loss was also recorded

at 80 °C, corresponding to a compound not detected by XRD, and thus amorphous or poorly crystallized.

3.2.3. Identification of the amorphous borate mineral precipitating at early age

Complementary experiments were performed in order to identify this compound. The pore solution was extracted by pressing the cement paste and characterized for its pH and chemical composition (Fig. 5). After an abrupt decrease from 11.6 to 11.0 at the very beginning of hydration, the pH showed little variation as long as gypsum was present, slightly decreasing from 11.0 to 10.75. About nine tenths of the borate ions were rapidly depleted. The solution also comprised high contents of sulfates (between 300 and 400 mmol/L), resulting from the progressive dissolution of gypsum, but its calcium concentration remained much lower (close to 20 mmol/L). The precipitation of an amorphous or poorly crystallized borate mineral containing calcium could be assumed from these results. It could also explain the rapid stiffening of the cement paste observed experimentally shortly after mixing.

The formation of a calcium borate with possible $\text{C}_2\text{B}_3\text{H}_8$ stoichiometry has already been postulated to explain the strong retarding effect of borate ions on OPC hydration [26]. However, the cement paste investigated in this study also comprised high sodium contents and thermodynamic calculations of the most stable phase assemblage rather predicted the precipitation of ulexite, a mixed borate mineral containing sodium and calcium ($\text{NaCa}[\text{B}_5\text{O}_6(\text{OH})_6](\text{H}_2\text{O})_5$). The modeled phase evolution occurring when a simplified cement comprising ye'elimite and gypsum only was hydrated in the presence of the sodium borate solution is indeed shown in Fig. 6-a.

When ye'elimite began to dissolve, the pore solution pH dropped from 12.2 to 10.8. Some gypsum was consumed and ulexite precipitated. Then, the pH remained stable at 10.8, AH_3 and an AFt-type phase (ettringite) precipitated while gypsum was progressively consumed. It should be noted that the thermodynamic database did not include any data concerning the solid solution between the 4Boro-AFt phase and

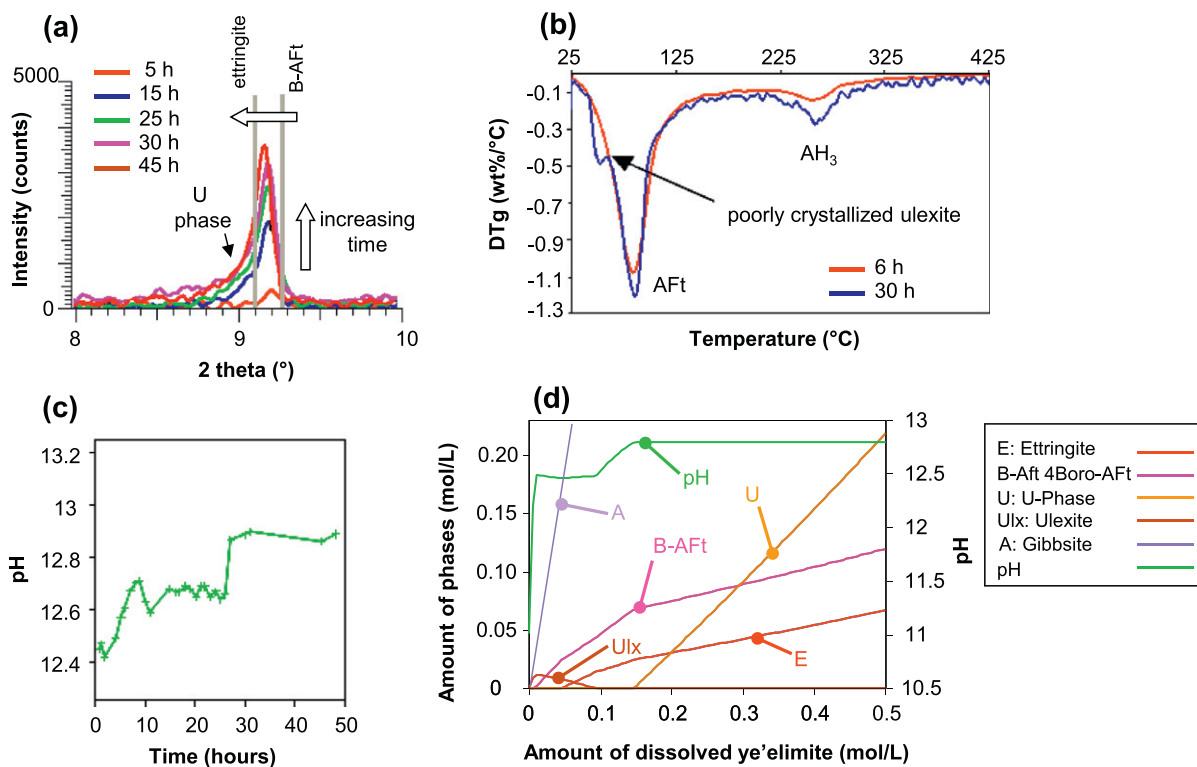


Fig. 9. Hydration of a CSA cement without gypsum in the presence of a sodium borate solution ($[\text{B}]_{\text{tot}} = 1 \text{ mol/L}$, $\text{pH} = 11$, $w/c = 0.6$; $T = 20 \text{ }^\circ\text{C}$). (a) Mineralogical evolution assessed by X-ray diffraction. (b) TGA analysis of two samples aged 6 h and 30 h. (c) Evolution of the pore solution pH with time. (d) Thermodynamic modeling of the hydrate assemblage formed by the progressive dissolution of ye'elimite in an aqueous suspension initially containing 1 mol/L of H_3BO_3 , and 960 mmol/L of NaOH.

ettringite, and only the pure phases could precipitate in this calculation. Exhaustion of gypsum was accompanied by a pH increase up to 12.7, and by the destabilization of ulexite which began to dissolve. Finally, once ulexite was fully depleted, the U-phase formed and the pH stabilized at 12.8. This simulation seemed rather consistent with the experiment: the pH variation was well reproduced, as well as the precipitation of AH_3 and the AFt-type phase, followed by the formation of the U-phase.

Even if ulexite could not be identified with certainty in the cement paste, assuming its transient precipitation during the period of low thermal activity seemed realistic for three reasons.

- (i) The saturation indexes of the solid phases were calculated using the concentrations of the aqueous species measured in the extracted interstitial solutions (Fig. 6-b). As long as gypsum was present, the aqueous phase was supersaturated with respect to gypsum, aluminum hydroxide and ettringite. Among the borate minerals (hexahydroborite, inyoite, borax, nobleite, sborgite, ulexite), ulexite exhibited the highest saturation index which was very close to zero, and thus to equilibrium, during this period.
- (ii) Some ulexite was synthesized according to Casabonne's protocol [27] by mixing calcium hydroxide and boric acid in demineralized water with a B/Ca molar ratio of 9, and by setting the pH to 10 by an addition of sodium hydroxide. A white and gel-like compound precipitated instantaneously. Its X-ray diffraction pattern, directly recorded on the suspension, mainly comprised two diffusion peaks at $2\theta = 29.2^\circ$ and 42.9° , which confirmed its poor crystallinity (Fig. 7-a). However, some diffraction peaks of very weak intensity were also observed at $2\theta = 7.1^\circ$, 21.0° and 30.9° , indicating the presence of ulexite traces. Drying the sample using isopropanol mainly yielded well crystallized ulexite (Fig. 7-c), with small amounts of portlandite (CH) and traces of pentahydroborite (CBH_5) and frolovite (CBH_4). The composition of the gel-like compound was determined by mass balance from the analysis of the aqueous phase in contact. The B/Ca and Na/Ca ratios were found to be respectively 4.9 ± 0.1 and 0.98 ± 0.02 , which fits rather well with the stoichiometry of ulexite ($\text{NaCa}[\text{B}_5\text{O}_6(\text{OH})_6](\text{H}_2\text{O})_5$). ESEM observations revealed a fibrillar morphology (Fig. 7-b), also reported for ulexite. The local borate organization in the gel-like product was also compared to that in well crystallized ulexite (Fig. 7-d). Both compounds exhibited the same ^{11}B MAS-NMR spectra, with two main peaks for chemical shifts in the range [18.5; 14] ppm and [3.5; 1.5] ppm which were characteristic of tricoordinated and tetraordinated boron atoms respectively. ^{11}B (80.22% naturally abundant) is a half-integer nucleus ($I = 3/2$) that possesses a quadrupolar momentum. This gives rise to a quadrupolar interaction, the amplitude of which strongly depends on the distortion of the site compared to the cubic symmetry. When this interaction is strong, the second-order terms of the interactions are only partially averaged by MAS, and this results in a characteristic lineshape that can be seen in Fig. 7-d for the B[III] sites. The splitting of the signal induces an experimental broadening and additionally shifts the peak to the lower ppm region [38–40]. On the contrary, for tetrahedral B[IV] sites, the higher symmetry corresponds to a small quadrupolar coupling constant, and the signals are nearly Gaussian [41,42]. The shoulder on the left side of the peak at [3.5; 1.5] ppm indicated two types of B[IV] sites, which is in good agreement with the structure reported for ulexite by Gode and Kuka [28]. From these experiments, it was concluded that the formation of well crystallized ulexite could be preceded by the rapid precipitation of a compound with the same stoichiometry, but with very poor organization at long distance, making it difficult to detect by X-ray diffraction. This compound was subsequently considered as ulexite.
- (iii) The solid phase of the one-day old cement paste hydrated in the

presence of the sodium borate solution was analyzed by ^{11}B MAS-NMR (Fig. 8). As for ulexite, the spectrum exhibited two peaks at [4; – 1.5] ppm and [19; 13] ppm, showing the presence of boron both in the tetrahedral and trigonal coordinations respectively. The ratio between the tetrahedral and trigonal sites was however much higher than that in ulexite. This could be explained by assuming the precipitation of two boron-containing phases: ulexite, but also the mixed AFt-type phase containing borate and sulfate anions, as previously evidenced by X-ray diffraction and thermogravimetry analysis (Figs. 3 and 4). Champenois et al. [24] have shown indeed that boron is tetrahedrally four-fold coordinated by oxygen in the crystal structure of the AFt phase. In comparison, the spectrum of a one-year old sample only exhibited one sharp peak characteristic of boron in tetrahedral coordination in the AFt phase. This spectroscopic analysis was thus consistent with the assumption of the transient precipitation of ulexite at early age in the cement paste hydrated in the presence of the sodium borate solution.

3.3. Transient precipitation of ulexite and hydration delay

Is there a relationship between the transient precipitation of poorly crystallized ulexite during the period of low thermal activity and the hydration delay caused by borate anions? To answer this question, the stability domain of ulexite was investigated as a function of two

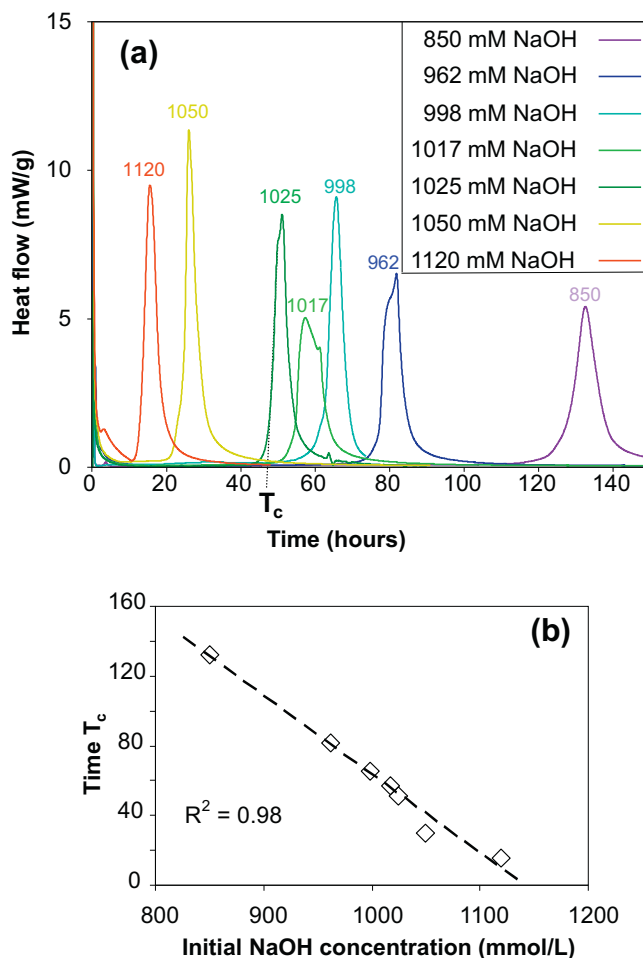


Fig. 10. Influence of the initial NaOH concentration in the mixing solution on the hydration of a CSA cement with 10% gypsum in the presence of a borate solution ($[\text{B}]_{\text{tot}} = 1 \text{ mol/L}$). (a) Heat flow recorded under isothermal conditions ($T = 25^\circ\text{C}$). (b) Correlation between parameter T_c and the NaOH concentration.

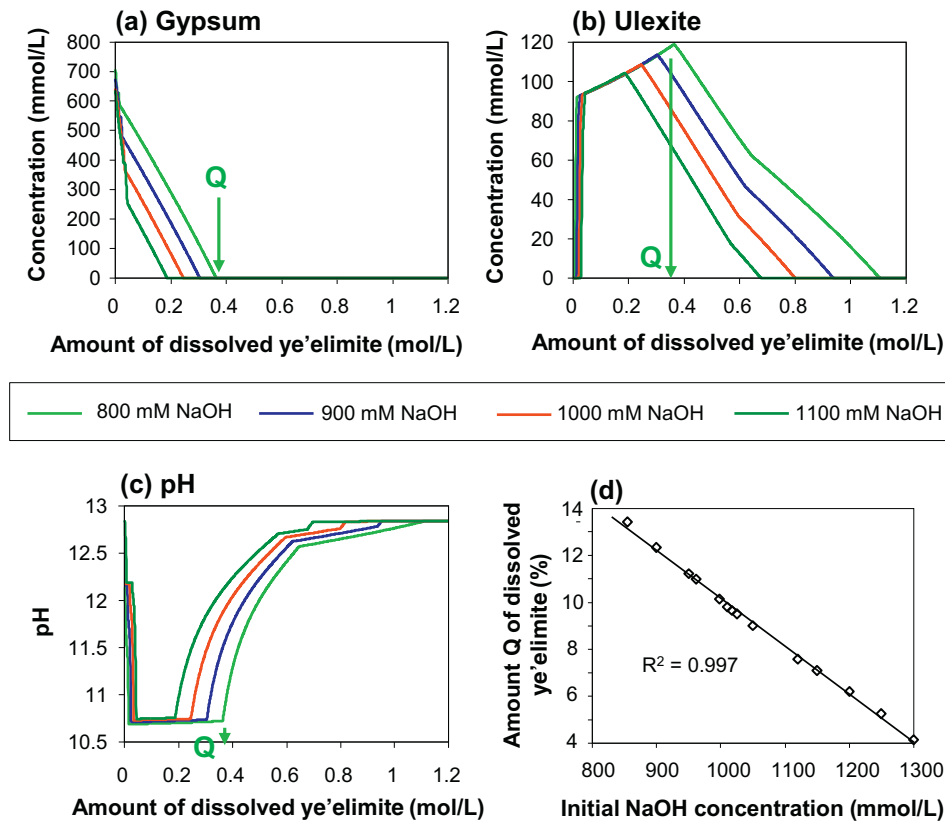


Fig. 11. Modeled evolution of gypsum (a), ulexite (b), and pH (c) with ongoing dissolution of ye'elimite in aqueous suspensions initially containing 970 mmol/L of gypsum, 1 mol/L of H₃BO₃, and variable concentrations of NaOH. (d) Correlation between parameter Q and the NaOH concentration.

parameters: the initial gypsum content of the cement, and the amount of sodium hydroxide added in the mixing solution.

3.3.1. Influence of the gypsum content on the stability of ulexite

A CSA cement paste free from gypsum was hydrated in the presence of the borate-containing solution. The precipitation of small amounts of aluminum hydroxide and of a mixed AFt-type phase incorporating sulfate and borate anions occurred during the period of low thermal activity (Fig. 9-a and b), and the pH stabilized at a value close to 12.6 (Fig. 9-c). Then, the pH increased to 12.8 and the precipitation of the U-phase was observed.

These experimental results were well reproduced by thermodynamic modeling of a simplified system in which ye'elimite was hydrated in the presence of the borate solution (Fig. 9-d). In particular, the agreement between the experimental and calculated pH values was excellent. The model still predicted the precipitation of ulexite at an early age, but this phase was more easily destabilized than in the presence of gypsum: the amount of ye'elimite to dissolve until ulexite exhaustion was 0.1 mol/L, instead of 0.8 mol/L when the system comprised 970 mmol/L gypsum (see Fig. 6-a). This decreased stability of ulexite in the absence of gypsum could be explained by the higher pH of the system during the first stage of hydration: instead of being buffered at 10.8, the pH was rapidly raised to 12.5. From a kinetic point of view, it was shown in Fig. 1 that the retardation of CSA cement hydration in the presence of borate anions was strongly reduced in the absence of gypsum.

3.3.2. Influence of the sodium hydroxide content on the stability of ulexite

The mixing solution which mimicked the radioactive waste was a boric acid solution ($[B]_{\text{tot}} = 1 \text{ mol/L}$) with a pH set to 11 by adding sodium hydroxide. The influence of a variation in the NaOH content on CSA cement hydration was investigated at a constant boron concentration. From the kinetic point of view, increasing the NaOH content

accelerated cement hydration, as shown by microcalorimetric experiments (Fig. 10-a).

The duration of the period of low thermal activity was characterized by defining parameter T_c as the intercept between the tangent to the first inflexion point of the heat flow peak and the x axis. This characteristic time T_c , which corresponded to gypsum exhaustion as shown in Section 3.2, decreased linearly when the NaOH concentration increased in the mixing solution (Fig. 10-b).

From the mineralogical point of view, the modeled phase evolution with ongoing hydration (Fig. 11) showed that increasing the initial NaOH concentration decreased the stability of ulexite: the amount of

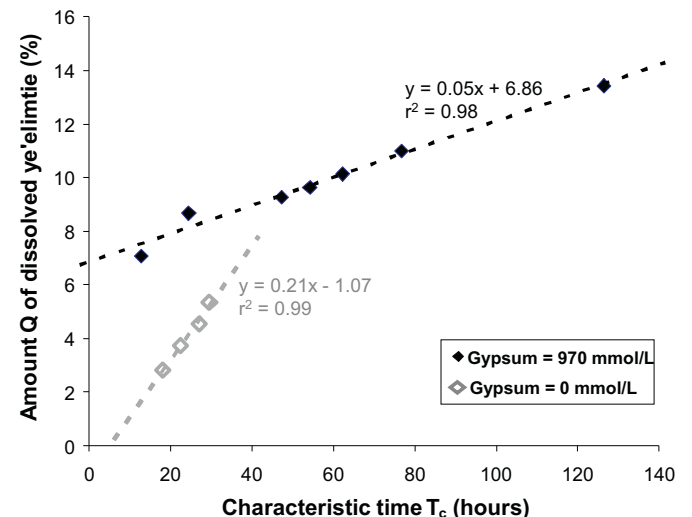


Fig. 12. Correlation between thermodynamic parameter Q and kinetic parameter T_c .

ye'elimite to be dissolved to exhaust gypsum and start ulexite dissolution, represented by parameter Q in Fig. 11, decreased linearly when the NaOH concentration increased in the mixing solution. The influent factor was the sodium concentration of the mixing solution rather than its hydroxide concentration. Fig. 11-c shows indeed that the pore solution pH before the exhaustion of gypsum stabilized to the same value of 10.7 whatever the initial pH: it was governed by the equilibria between the solid phases and the solution. On the contrary, the sodium concentration directly influenced the stability of ulexite and the U-phase.

Plotting thermodynamic parameter Q versus kinetic parameter T_c showed their strong correlation (Fig. 12), meaning that the transient precipitation of ulexite played a key role in controlling the reactivity of CSA cement at an early age. The higher the amount of precipitated ulexite, the higher the amount of ye'elimite needed to be dissolved for destabilizing this phase, the longer the duration of the period of low thermal activity, and thus the longer the hydration delay. The slope of the curves plotting Q versus T_c represented the average dissolution rate of ye'elimite during the period of low thermal activity. It remained constant, meaning that it was controlled by a pseudo-stationary state. The latter depended on the cement composition: the dissolution rate of ye'elimite was higher in the absence of gypsum than with 10% gypsum.

4. Conclusion

Hydration of CSA cements containing 0 to 20% gypsum in the presence of a concentrated sodium borate solution was investigated at an early age. The borate ions retarded CSA cement hydration, all the more since the gypsum content of the binder was high. They were shown to be rapidly partially depleted from the mixing solution and precipitated into two hydrates: (i) ulexite with very poor crystallinity, which formed transiently during the period of low thermal activity, and (ii) a mixed AFT-type phase containing borates and sulfates, which tended to get richer in sulfates with time.

The transient precipitation of ulexite revealed to play a key role in the control of the cement reactivity at early age. The duration of the period of low thermal activity increased with the amount of ulexite precipitated, and the acceleration of cement hydration occurred only when this phase was destabilized and began to dissolve. It should be noted that other processes, such as slowing down of the dissolution of anhydrous cement phases, or poisoning of the precipitation of cement hydrates, might also be involved in the hydration delay, and will have to be investigated in a dedicated study.

Preventing, or limiting, the precipitation of ulexite was found to be an efficient way to decrease the retardation of CSA cement hydration due to borate ions. This could be achieved by decreasing the gypsum content of the cement, or by increasing the sodium content of the mixing solution. The next important stage will be to determine the long-term properties of the resulting materials.

Acknowledgments

The authors greatly acknowledge Laurent Petit from Electricité de France (EDF) for his support of the study, and Johann Ravaux (CNRS/ICSM) for his help concerning ESEM observations.

References

- [1] E. Gartner, Industrially interesting approaches to "low-CO₂" cements, *Cem. Concr. Res.* 34 (2004) 1489–1498.
- [2] M.C.G. Juenger, F. Winnefeld, J.L. Provis, J.H. Ideker, Advances in alternative cementitious binders, *Cem. Concr. Res.* 41 (2011) 1232–1243.
- [3] A. Klein, G.E. Troxell, Studies of calcium sulfoaluminate admixture for expansive cements, *ASTM Proceedings* 1958. (986).
- [4] R.K. Mehta, Investigation on the products in the system $C_4A_3S-CaSO_4-CaO-H_2O$, Annual Meeting of the Highway Research Board Proceedings 1965. 328–352.
- [5] I. Odler, Special inorganic cements, in: A. Bentur, S. Mindness (Eds.), *Modern Concrete Technology*, 8, E&F.N. Son, London, 2000, pp. 69–87.

- [6] T. Sui, Y. Yao, Recent progress in special cements in China, Proc. 11th International Conference on The Chemistry of Cement, Durban, South Africa, 11–16 May, 2003, pp. 2028–2032.
- [7] O. Andac, F.P. Glasser, Microstructure and microchemistry of calcium sulfoaluminate cement, *Mater. Res. Soc. Symp. Proc.* 370 (1995) 132–142.
- [8] F.P. Glasser, L. Zhang, High-performance cement matrices based on calcium sulfoaluminate–belite compositions, *Cem. Concr. Res.* 31 (2001) 1881–1886.
- [9] V. Albino, R. Cioffi, M. Marroccoli, L. Santoro, Potential application of ettringite generating systems for hazardous waste stabilization, *J. Hazard. Mater.* 51 (1996) 241–252.
- [10] R. Berardi, R. Cioffi, L. Santoro, Matrix stability and leaching behaviour in ettringite-based stabilization systems doped with heavy metals, *Waste Manag.* 17 (1997) 535–540.
- [11] J. Pera, J. Ambrose, M. Chabannet, Valorization of automotive shredder residue in building materials, *Cem. Concr. Res.* 34 (2004) 557–562.
- [12] S. Pessysson, J. Pera, M. Chabannet, Immobilization of heavy metals by calcium sulfoaluminate cement, *Cem. Concr. Res.* 35 (2005) 2261–2270.
- [13] S. Berger, C. Cau Dit Coumes, P. Le Bescop, D. Damidot, Hydration of calcium sulfoaluminate cement by a ZnCl₂ solution: investigation at early age, *Cem. Concr. Res.* 30 (2009) 1180–1187.
- [14] S. Berger, C. Cau Dit Coumes, P. Le Bescop, D. Damidot, Stabilization of ZnCl₂-containing wastes using calcium sulfoaluminate cement: cement hydration, strength development and volume stability, *J. Hazard. Mater.* 194 (2011) 256–267.
- [15] S. Berger, C. Cau Dit Coumes, J.B. Champenois, T. Douillard, P. Le Bescop, G. Aouad, D. Damidot, Stabilization of ZnCl₂-containing wastes using calcium sulfoaluminate cement: leaching behaviour of the solidified waste form, mechanisms of zinc retention, *J. Hazard. Mater.* 194 (2011) 268–276.
- [16] Q. Sun, J. Wang, Cementation of radioactive borate liquid waste produced in pressurized water reactors, *Nucl. Eng. Des.* 240 (2010) 3660–3664.
- [17] Q. Sun, J. Li, J. Wang, Effect of borate concentration on solidification of radioactive wastes by different cements, *Nucl. Eng. Des.* 241 (2011) 4341–4345.
- [18] Q. Sun, J. Li, J. Wang, Solidification of borate radioactive resins using sulfoaluminate cement blending with zeolite, *Nucl. Eng. Des.* 241 (2011) 5308–5315.
- [19] J.B. Champenois, C. Cau Dit Coumes, P. Le Bescop, D. Damidot, Immobilisation of borates anions using calcium sulfoaluminate cements, in: F. Bart, C. Cau Dit Coumes, F. Frizon, S. Lorente (Eds.), *Cement-based Materials for Nuclear Waste Storage*, Springer, New York, USA, 2013, pp. 203–213.
- [20] R. Wenda, H.J. Kuzel, Incorporation of B³⁺ into calcium aluminate hydrate, *Fortschr. Mineral.* 61 (1983) 217–218.
- [21] L.J. Csetenyi, F.P. Glasser, Borate substituted ettringites, *Mat. Res. Soc. Symp. Proc.* 294 (1993) 273–278 (MRS Publ., Pittsburgh, PA, USA).
- [22] J.V. Bothe Jr., P.W. Brown, Phase formation in the system CaO–Al₂O₃–B₂O₃–H₂O at 23 ± 1 °C, *J. Hazard. Mater.* B 63 (1998) 199–210.
- [23] H. Poellmann, S. Auer, H.J. Kuzel, Solid solution of ettringite – part II – incorporation of [B(OH)₄]⁻ and CrO₄²⁻ in 3CaO·Al₂O₃·3CaSO₄·32H₂O, *Cem. Concr. Res.* 23 (1993) 422–430.
- [24] J.B. Champenois, A. Mesbah, C. Cau Dit Coumes, G. Renaudin, F. Leroux, C. Mercier, B. Revel, D. Damidot, Crystal structures of Boro-AFm and Boro-AFT phases, *Cem. Concr. Res.* 42 (2012) 1362–1370.
- [25] P.H. Kemp, *The Chemistry of Borates*, a Review, Borax Consolidated, London, 1956. 90.
- [26] C. Roux, Conditionnement par des liants hydrauliques de concentrats boratés radioactifs: formulation et caractérisation, Orsay Paris Sud University, 1989. (PhD thesis in French).
- [27] J.M. Casabonne Masonnave, Immobilisation des radioéléments provenant de déchets nucléaires sous forme de composés insolubles ou par réaction d'échange dans une matrice béton, University of Burgundy, 1987. (PhD thesis in French).
- [28] G.K. Gode, P.Y. Kuka, Synthesis of calcium borates from aqueous solutions, *Z. Neorganicheskoj Khimii* 15 (1970) 1176–1181.
- [29] S. Berger, C. Cau Dit Coumes, P. Le Bescop, D. Damidot, Influence of a thermal cycle at early age on the hydration of calcium sulfoaluminate cements with variable gypsum contents, *Cem. Concr. Res.* 41 (2011) 149–160.
- [30] D. Massiot, F. Fayon, M. Capron, I. King, S. Le Calvé, B. Alonso, J.O. Durand, B. Bujoli, Z. Gan, G. Hoatson, Modelling one and two-dimensional solid-state NMR spectra, *Magn. Reson. Chem.* 40 (2002) 70–76.
- [31] J. Van der Lee, Thermodynamic and mathematical concepts of CHESS, Technical Report LHM/RD/98/39, 1998, p. 99.
- [32] D. Damidot, B. Lothenbach, D. Herfort, F.P. Glasser, Thermodynamics and cement science, *Cem. Concr. Res.* 4 (2011) 679–695.
- [33] J.B. Champenois, Etude de l'hydratation de ciments sulfo-alumineux par des solutions de borate de sodium: de la spéciation du bore au retard à l'hydratation, Montpellier II University, France, 2012, p. 248 PhD thesis [in French].
- [34] T. Matschei, B. Lothenbach, F.P. Glasser, Thermodynamic properties of Portland cement hydrates in the system CaO–Al₂O₃–SiO₂–CaSO₄–CaCO₃–H₂O, *Cem. Concr. Res.* 37 (2007) 1379–1410.
- [35] F. Winnefeld, S. Barlag, Calorimetric and thermogravimetric study on the influence of calcium sulphate on the hydration of ye'elimite, *J. Therm. Anal. Calorim.* 101 (2010) 949–957.
- [36] J.B. Champenois, C. Cau Dit Coumes, A. Poulesquen, P. Le Bescop, D. Damidot, Beneficial use of a cell coupling rheometry, conductimetry and calorimetry to investigate the early age hydration of calcium sulfoaluminate cement, *Rheol. Acta.* 52 (2013) 177–187.
- [37] G. Li, P. Le Bescop, M. Moranville, The U phase formation in cement-based systems containing high amounts of Na₂SO₄, *Cem. Concr. Res.* 26 (1996) 27–33.
- [38] G.L. Turner, K.A. Smith, R.J. Kirkpatrick, E. Oldfield, Boron-11 nuclear magnetic resonance spectroscopic study of borate and borosilicate minerals and of a borosilicate glass, *J. Magn. Reson.* 67 (1986) 544–550.

- [39] P.J. Bray, J.O. Edwards, J.G. O'Keefe, V.F. Ross, I. Tatsuzaki, Nuclear magnetic resonance studies of B11 in crystalline borates, *J. Chem. Phys.* 35 (1961) 435–442.
- [40] S. Kroeker, J.F. Stebbins, Three-coordinated boron-11 chemical shifts in borates, *Inorg. Chem.* 40 (2001) 6239–6246.
- [41] C. Gervais, F. Babonneau, High resolution solid state NMR investigation of various boron nitride preceramic precursors, *J. Organomet. Chem.* 657 (2002) 75–82.
- [42] K.P. Peil, L.G. Galya, G. Marcellin, Acid and catalytic properties of non stoichiometric aluminium borates, *J. Catal.* 115 (1989) 441–451.
- [43] G.G.N. Manov, N.J. Delollis, P.W. Lindvall, S.F. Acree, Effect of sodium chloride on the apparent ionization constant of boric acid and the pH values of borate solutions, *J. Res. Natl. Bur. Stand.* 36 (1946) 543–558.
- [44] B.B. Owen, The dissociation constant of boric acid from 10 to 50 °C, *J. Am. Chem. Soc.* 56 (1934) 1695–1697.
- [45] B.B. Owen, E.J. King, The effect of sodium chloride upon the ionization of boric acid at various temperatures, *J. Am. Chem. Soc.* 65 (1943) 1612–1620.
- [46] C.F. Baes, R.E. Mesmer, The thermodynamics of cation hydrolysis, *Am. J. Sci.* 281 (1981) 935–962.
- [47] N. Ingri, Equilibrium studies of polyanions. 8. On the first equilibrium steps in the hydrolysis of boric acid, a comparison between equilibria in 0.1 M and 3.0 M NaClO₄, *Acta Chem. Scand.* 16 (1962) 439–453.
- [48] R.K. Momii, N. Nachtrieb, Nuclear magnetic resonance study of borate–polyborate equilibria in aqueous solution, *Inorg. Chem.* 6 (1967) 1189–1192.
- [49] N. Ingri, Equilibrium studies of polyanions. 10. On first equilibrium steps in acidification of B(OH)₄, an application of self-medium method, *Acta Chem. Scand.* 17 (1963) 573–581.
- [50] N. Ingri, Equilibrium studies of polyanions. 11. Polyborates in 3.0 M NaBr, 3.0 M LiBr and 3.0 M KBr, a comparison with data obtained in 3.0 M NaClO₄, *Acta Chem. Scand.* 17 (1963) 581–589.
- [51] L. Maya, Identification of polyborate and fluoropolyborate ions in solution by Raman spectroscopy, *Inorg. Chem.* 15 (1976) 2179–2184.
- [52] R.H. Byrne, D.R. Kester, Inorganic speciation of boron in seawater, *J. Mar. Res.* 32 (1974) 119–127.
- [53] E.J. Reardon, Dissociation constants for alkali earth and sodium borate ion pairs from 10 to 50 °C, *Chem. Geol.* 18 (1976) 309–325.
- [54] L.J. Cstetenyi, F.P. Glasser, Borate retardation of cement set and phase relations in the system Na₂O–CaO–B₂O₃–H₂O, *Adv. Cem. Res.* 25 (1995) 13–19.
- [55] J. Zhang, M. Klasky, B.C. Letellier, The aluminum chemistry and corrosion in alkaline solutions, *J. Nucl. Mater.* 384 (2009) 175–189.